

Disruption of LPA-LPAR1 pathway results in lung tumor growth inhibition by downregulating B7-H3 expression in fibroblasts

Fanyi Meng  | Zhiyue Yin | Feifei Lu | Weipeng Wang | Hongjian Zhang

College of Pharmaceutical Sciences, Soochow University, Suzhou, China

Correspondence

Fanyi Meng, College of Pharmaceutical Sciences, Soochow University, Suzhou 215123, China.
Email: fymeng@suda.edu.cn

Abstract

Background: Lysophosphatidic acids (LPAs) belong to a class of bioactive lysophospholipids with multiple functions including immunomodulatory roles in tumor microenvironment (TME). LPA exerts its biological effects via its receptors that are highly expressed in fibroblasts among other cell types. As cancer-associated fibroblasts (CAFs) are a key component of the TME, it is important to understand LPA signaling and regulation of receptors in fibroblasts or CAFs and associated regulatory roles on immunomodulation-related molecules.

Methods: Cluster analysis, immunoblotting, real-time quantitative-PCR, CRISPR-Cas9 gene editing system, immunohistochemical staining, coculture model, and in vivo xenograft model were used to investigate the effects of LPA-LPAR1 on B7-H3 in tumor promotion of CAFs.

Results: In this study, we found that LPAR1 and CD276 (B7-H3) were generally highly expressed in fibroblasts with good expression correlation. LPA induced B7-H3 up-expression through LPAR1, and stimulated fibroblasts proliferation that could be inhibited by silencing LPAR1 or B7-H3 as well as small molecule LPAR1 antagonist (Ki16425). Using engineered fibroblasts and non-small cell lung carcinoma (NSCLC) cell lines, subsequent investigations demonstrated that CAFs promoted the proliferation of NSCLC in vitro and in vivo, and such effect could be inhibited by knocking out LPAR1 or B7-H3.

Conclusion: The present study provided new insights for roles of LPA in CAFs, which could lead to the development of innovative therapies targeting CAFs in the TME. It is also reasonable to postulate a combinatory approach to treat malignant fibrous tumors (such as NSCLC) with LPAR1 antagonists and B7-H3 targeting therapies.

KEYWORDS

B7-H3, cancer-associated fibroblasts, LPAR1, lysophosphatidic acid, non-small cell lung cancer

INTRODUCTION

Initiation, growth, progression and metastasis of cancer lead to extensive changes and structural alterations in host tissues, resulting in the formation of a complex tumor stroma, also known as the tumor microenvironment (TME).¹ In general, the TME consists of extracellular matrix (ECM) components and a variety of cell types, including immune cells, fibroblasts, and vascular endothelial cells. Populations of fibroblasts found in primary and metastatic cancers, collectively referred to as cancer-associated fibroblasts (CAFs),

have been implicated in tumor initiation, progression, and metastasis.² CAFs could support tumor growth through multiple mechanisms, whereby CAFs not only deposit ECM but also produce matrix remodeling enzymes, thereby promoting tumor invasion, metastasis, and resistance to therapies.^{3–5} In addition, CAFs can promote tumor growth and invasion by secreting various cytokines, exosomes, and growth factors, such as leukemia inhibitory factor (LIF) and growth differentiation factor 15 (GDF15).^{6,7}

CAFs reside in almost all solid tumors and associate with poor prognosis of invasion in a variety of cancers.^{3,8} In

malignant fibrous tumors with high CAFs density, such as pancreatic cancer, breast cancer, and non-small cell lung cancer (NSCLC), the multiple tumor-promoting functions that CAFs exhibit during tumor progression make them attractive therapeutic targets for oncotherapy.⁹ For example, fibroblast activation protein (FAP) is one of the most viable and clinically useful markers of CAFs. In multidrug-resistant mouse models, oral FAP DNA vaccine induced CD8T cell-mediated killing of CAFs and successfully inhibited primary tumor growth as well as colon and breast carcinoma metastasis.¹⁰ Similarly, adoptive transfer of FAP-specific chimeric antigen receptor (CAR) T cells, inhibited the growth of connective tissue proliferative human lung cancer xenografts and syngeneic murine pancreatic cancer.¹¹ While many drugs targeting key regulators of CAFs are undergoing clinical and preclinical evaluation, many of the published clinical trials have yielded disappointing results.⁹ Therefore, it is prudent to conduct more in-depth research on the molecular mechanisms of CAFs, especially how CAFs interact with tumor cells and through what mechanism(s) CAFs promote the progression of tumor and poor patient prognosis.

Lysophosphatidic acids (LPAs) are a class of bioactive lysophospholipid molecules with multiple functions in both developmental and pathological conditions.¹² LPA binds six primary LPA transmembrane receptors (LPAR1 to LPAR6) with varying affinities that are coupled to four different heterotrimeric G proteins (G12/13, Gq/11, Gi/o, and Gs) and trigger various downstream signaling cascades.^{12,13} Consequently, LPA could mediate cellular events such as cell proliferation, survival, apoptosis, migration, fibrosis, inflammation, and tumor progression.¹⁴ Recently, LPA has been proposed to promote tumor immune invasion via a mechanism similar to that of CTLA-4 and PD-1.¹⁵ Specifically, LPA via LPAR5 has been shown to modulate CD8 T cell metabolism and impair antitumor immunity.¹⁶ It has also been suggested that tumor-derived LPA accelerates the progression of hepatocellular carcinoma by promoting the differentiation of peritumoral fibroblasts into myofibroblasts.¹⁷ In addition, LPA stimulates glycolysis in both the normal and cancer-associated fibroblasts along with the expression of CAF-specific phenotypic markers.¹⁸ However, there have been no studies on whether LPA regulates tumor immunity by mediating immune checkpoint protein on CAFs. The mechanisms of how LPA regulates CAFs to promote tumor progression are also still unclear.

In this study, we first examined the expression correlation among LPA receptors and several key checkpoint proteins in fibroblasts based on the literature and observed a good correlation between LPAR1 and CD276 (B7-H3). This observation was then verified using relevant cell lines including fibroblasts and lung cancer cells. Next, we evaluated effects of LPA (18:1) on B7-H3 expression in HLF-a and MRC-5 cells, followed by investigations on roles of LPAR1 on B7-H3 expression using siRNAs knockdown or small molecule LPAR1 antagonist (Ki16425). Further in vitro experiments interrogated effects of LPA, LPAR1 and B7-H3 on fibroblasts proliferation under various conditions. Finally, we employed engineered fibroblasts cell lines with

LPAR1 or B7-H3 knockout and examined related effects on tumor cell growth in vitro and in vivo. It is expected that the present study will provide new insights for the role of CAFs in tumor proliferation and aid the development of innovative therapies targeting LPAR1 and B7-H3 on CAFs for better clinical outcomes of malignant fibrous cancers.

METHODS

Cell culture and reagents

Cell lines such as HFL-1 (CCL-153), HLF-a (CCL-199), LL97A (CCL-191), MRC-5 (CCL-171), A549 (CRM-CCL-185), NCI-H460 (HTB-177), and NCI-H1703 (CRL-5889) were purchased from the American Type Culture Collection (Manassas). The A549-eGFP-Puro (CL079) cells were purchased from Biofeng and were cultured in media recommended by the vendor containing 10% fetal bovine serum (FBS: 10099141C, Gibco) with penicillin (100 U/mL) and streptomycin (100 µg/mL). The cultures were incubated at 37°C at 5% CO₂. LPA (18:1, 857130P) was purchased from Sigma. All LPAR siRNAs were synthesized by GenePharma. LPAR1 antagonist Ki16425 (Debio 0719) was purchased from MCE. Dulbecco's modified Eagle medium (DMEM) (C11995500), MEM (11095098), F12K (21127022) and RPMI 1640 (C11875500) cell culture media were purchased from Gibco.

Cell transfection

To investigate the regulatory role of siRNAs in gene expression and proliferation, synthetic siRNAs or siRNAs control (Table S1) were transfected into fibroblasts and NSCLC cell lines using lipofectamine 3000 (L3000015, Invitrogen) in Opti-MEM (31 985 070, Gibco) without serum according to the manufacturer's instructions for 48 h (RNA analysis) or 72 h (protein analysis).

RNA quantification

For quantitative real-time-polymerase chain reaction (qRT-PCR), total RNA was isolated from cells using TRIzol reagent (9109, Takara). The total RNA extracted was reverse transcribed into cDNA using NxGen M-MuLV reverse transcriptase (28 025 021, Invitrogen). qRT-PCR was performed using qRT-PCR master mix (1 725 272, Bio-Rad) and primers (Table S1) on CFX96 Touch real-time PCR system (Bio-Rad). RNA expression levels were normalized to those of glyceraldehyde 3-phosphate dehydrogenase (GAPDH).

Western blot

Total proteins from cells were extracted using radioimmunoprecipitation assay (RIPA) lysis buffer (P0013B, Beyotime). Protein concentrations were determined using the

Pierce BCA protein assay kit (23227, Thermo). Aliquots of 20 µg proteins were separated on a 10% SDS-PAGE gel and electro-transferred onto a polyvinylidene difluoride (PVDF) membrane (ISEQ00010, Merck Millipore). After blocking using 5% skim milk, the membrane was incubated with primary antibody at 4°C overnight and subsequently with the corresponding secondary antibody (Santa Cruz Biotech) for 1 h at room temperature. The membrane was then developed using Clarity Western ECL substrates (WBKLS0500, Merck Millipore) and visualized with a ChemiDoc MP Imaging System (Bio-Rad). Protein expression was normalized with β-tubulin or β-actin expression. The antibodies against LPAR1 (#3U1Q0), β-tubulin (2G10) and FAP (F11-24) were purchased from Invitrogen. The antibodies against α-SMA (D4K9N) and β-actin (8H10D10) were purchased from Cell Signaling Technology. The antibodies against B7-H3 (#376769) were purchased from Santa Cruz Biotech.

Immunohistochemistry (IHC)

Sections were deparaffinized in xylene, hydrated in ethyl alcohol and washed in tap water. Fibroblast activation protein and α-smooth muscle actin staining with antibodies against FAP (F11-24) and α-SMA (D4K9N) was carried out as previously described. A Sirius red total collagen detection kit (#9062) was purchased from Chondrex. The adjacent sections were stained with diaminobenzidine or 3-amino-9-ethylcarbazole in an Envision System (Dako). Slides were viewed and imaged on a microscope system (Olympus). Two pathologists performed an independent review of the IHC results.

Cell counting kit-8 assay

Cell proliferation was measured using a CCK-8 assay kit (CK04, Dojindo). Approximately 3000 cells were plated into each well of a 96-well plate (3599, Corning) and treated with LPA (18:1), Ki16425 or transfected with 50 nM siRNAs or siRNA control using lipofectamine 3000. After 72 h, 10 µL CCK-8 was added into 90 µL culture medium. Cells were subsequently incubated for 15 min at 37°C and the optical density was measured at 450 nm using M3 SpectraMax microplate reader (Biotek).

CRISPR knockout and single clone selection

CRISPR targeting sequences for CD276 (CACAGGGCAA-CGCATCCCTG) and LPAR1 (CCACACACGGATGAG--CAACCG) were cloned into either LentiCRISPRv2 vector (Addgene, #52961). HLF-a was cotransfected with the plasmids LentiCRISPRv2-gRNA, pMD2.G (Addgene, #12259), and psPAX2 (Addgene, #12260) by PEI Max to produce a lentivirus. After 48 h of infection, the cells were sorted and

subcloned to generate single cell clones at a low density (200 cells/10 cm plate). After 14 days of post-puromycin (2 µg/mL) selection, KO cells were verified by western blotting.

Tumor xenograft model

Protocols for animal husbandry and experiments were approved by the Institutional Animal Care and Use Committee at Soochow University. All animal experiments complied with the ARRIVE guidelines and were carried out in accordance with the National Institutes of Health guide for the care and use of laboratory animals (NIH publication no. 8023, revised 1978). Male nude mice were purchased from SLAC International (Shanghai, China). All animals were kept in specific-pathogen-free (SPF) conditions in the Animal Resource Center at Soochow University. Athymic male SCID mice (BALB/c-*Foxn1*^{nu}/Nju, Gem Pharmatech, China) at about 4–6 weeks were used to explore the effect of fibroblasts on the growth of NSCLC. Approximately 1×10^5 A549 or H1703 cells were collected and mixed with matrigel (356 234, Corning) at a 1:1 ratio by volume and then injected alone or coinjected with 5×10^5 engineered fibroblasts (HLF-a^{wt}, HLF-a^{CD276-/-} or HLF-a^{LPAR1-/-}) into the lower back region of SCID mice. When tumors were palpable, mice were randomly divided into four groups ($n = 5$). Tumor volumes were measured using digital calipers, and all mice were euthanized when the progressing group had to be sacrificed due to tumor volume per IACUC standards. The tumor sizes and mouse bodyweights were nonblindly monitored every other day. The tumor size was evaluated according to the following equation:

$$\text{tumor size (mm}^3\text{)} = (\text{length} \times \text{width}^2)/2.$$

Statistical analysis

All statistical analysis was performed using GraphPad Prism 8 software. A student's *t* test was used to compare the two groups. The results are presented as mean ± SD, with $p < 0.05$ considered as statistically significant.

RESULTS

LPAR1 and CD276 (B7-H3) were generally highly expressed in fibroblasts

To explore the relationship between LPAR receptors and the B7 family of costimulatory molecules in fibroblasts. First, we performed cluster analysis of related genes in 38 fibroblasts from the Cancer Cell Line Encyclopedia (CCLE) database. The results are shown in Figure 1a, LPAR1 and CD276 (B7-H3) were significantly highly expressed in all 38 fibroblasts and showed a certain degree of expression correlation.

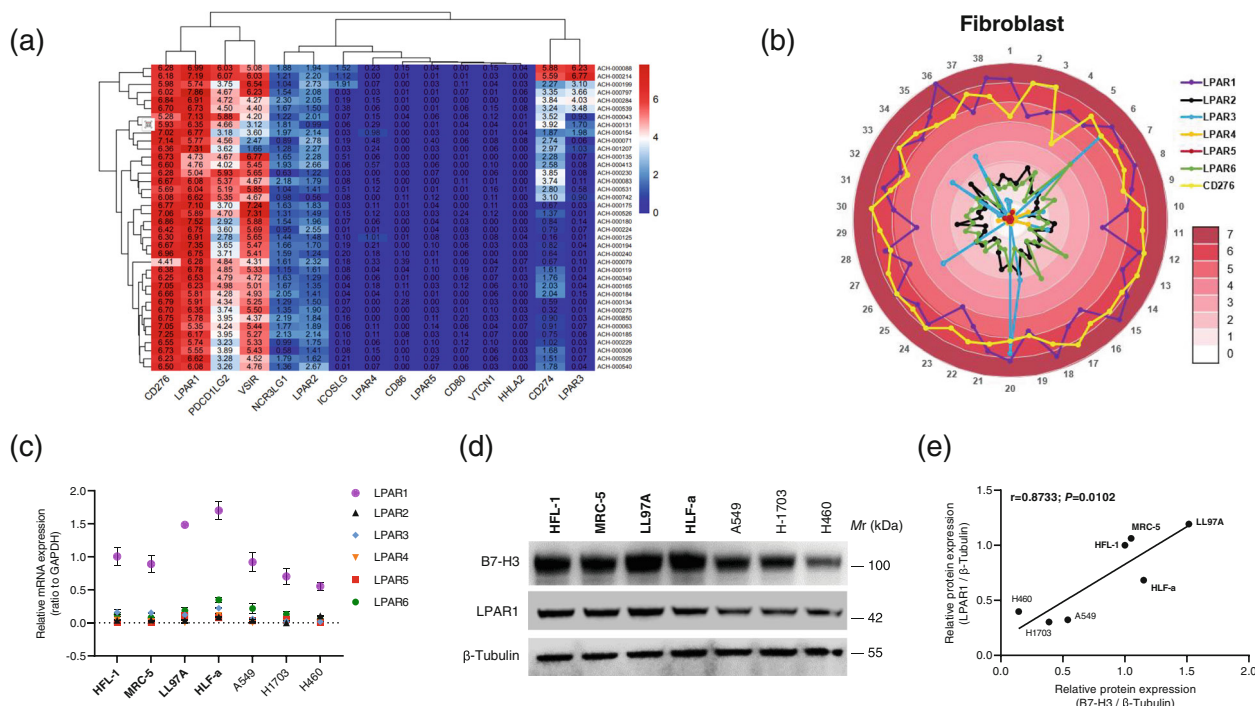


FIGURE 1 LPAR1 and CD276 (B7-H3) were generally highly expressed in fibroblasts. (a) Clustering analysis of the B7 gene family and LPAR gene family (blue = weaker, red = stronger). In the heat map, the rows represent the 38 fibroblasts from CCLE database (expression 22Q2 Public), and the columns represent the B7 gene family and LPAR gene family. (b) Radar plots demonstrated the differential expression of the LPAR gene family and CD276 in 38 fibroblasts from CCLE. (c) Real-time PCR data showed the relative mRNA expression of the LPAR gene family in HFL-1, MRC-5, LL97A, HLF-a, A549, H1703, H460 cell lines. (d) Western blot data showed the expression of B7-H3 and LPAR1 in HFL-1, MRC-5, LL97A, HLF-a, A549, H1703, H460 cell lines. (e) B7-H3 protein expression was positively correlated with LPAR1 protein expression in HFL-1, MRC-5, LL97A, HLF-a, A549, H1703, H460 cell lines. Data represent mean \pm SD. Significance was assessed by two-sided *t*-test. ****p* < 0.001; ***p* < 0.01; **p* < 0.05; ns, no significance.

Furthermore, the expression level of the other five LPA receptors was lower compared to LPAR1 in these 38 fibroblasts (Figure 1b). The correlation between the high expression of LPAR1 and CD276 (B7-H3) also showed fibroblast specificity that is not present in tumor cell lines (Figure 1SA). We then tested the mRNA and protein expression including human embryonic lung fibroblasts (HFL-1 and MRC-5), lung fibroblast derived from an idiopathic pulmonary fibrosis (IPF) patient (LL97A), lung fibroblast derived from NSCLC patient (HLF-a) and NSCLC cell lines (A549, H1703, and H460), and the results were consistent with the database (Figure 1c,d; Figure 1SB). Moreover, LPAR1 and B7-H3 in these seven cell lines showed a significant positive correlation at the protein levels (Figure 1e; $r = 0.8733$; $p = 0.0102$). The above results indicated that LPAR1 and B7-H3 were highly and specifically expressed in fibroblasts and showed a good expression correlation.

LPA-induced B7-H3 up-expression via LPAR1 in fibroblasts

Excessive secretion of LPA has been detected in pathological conditions and has been shown to induce an immunosuppressive environment in the TME of a variety of cancers.^{13,19} Therefore, to investigate whether LPA has a regulatory effect on the negative costimulatory molecule B7-H3 in fibroblasts, we first detected the expression of B7-H3 in MRC-5 and

HLF-a after treatment with LPA at different time points. As shown in Figure 2a, B7-H3 showed significant time-dependent up-regulation under LPA induction in both types of cells. Next, we designed small interfering RNAs for each of the six receptors of LPA and verified their functions (two siRNAs were designed for each LPA receptor. Figure 2b; Table S1). After transfection of the two cells separately, we found that only silenced LPAR1 reduced the expression of B7-H3 (the inhibition over 50% compared to the control) (Figure 2c). Moreover, when we stimulated with LPA and transfected the siRNA of LPAR1 simultaneously, the induced upregulated expression of B7-H3 was significantly reversed (Figure 2d). Finally, we used specific small molecule LPAR1 antagonist ki16425 (10 μ M) to block the LPA-LPAR1 signaling pathway in MRC-5 and HLF-a, and the same results were obtained as Figure 2c (Figure 2e). These findings confirmed that LPA upregulated the expression of B7-H3 through LPAR1, and silencing LPAR1 gene expression or blocking its signaling pathway both resulted in down-regulation of B7-H3 expression.

Silencing of LPAR1 or CD276(B7-H3) inhibited LPA-stimulated fibroblasts proliferation

The proliferation and migration of tumor cells induced by paracrine LPA has been confirmed by many studies, even in the absence of stromal growth factors.²⁰ However, the effect

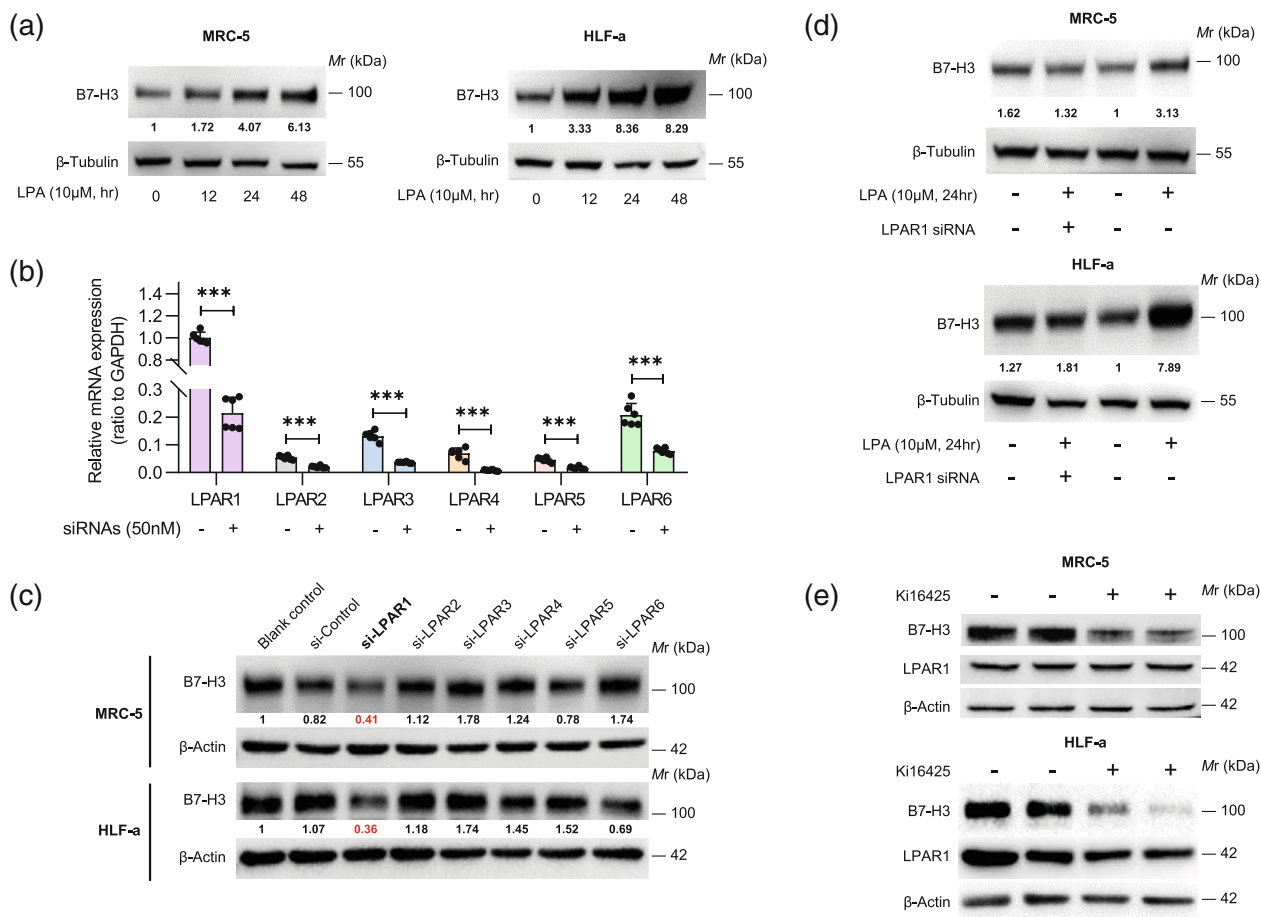


FIGURE 2 Lysophosphatidic acid (LPA)-induced B7-H3 up-expression via LPAR1 in fibroblasts. (a) Western blot data showed the expression of B7-H3 treated with LPA 18:1 (10 μM) for different times in MRC-5 and HLF-a cells. (b) Real-time PCR data showed the validation of siRNAs (50 nM). (c) Western blot data showed the expression of B7-H3 treated with LPA 18:1 (10 μM, 24 h) with or without LPAR1 siRNA (50 nM) in MRC-5 and HLF-a cells. (d) Western blot data showed the expression of B7-H3 treated with 10 μM Ki16425 in MRC-5 and HLF-a cells. Data represent mean ± SD. Significance compared to negative control was assessed by two-sided *t*-test. ****p* < 0.001; ***p* < 0.01; **p* < 0.05; ns, no significance.

of exogenous LPA on fibroblasts proliferation is still unclear. Therefore, to investigate whether LPA, LPAR1 or B7-H3 affected the proliferation of fibroblasts, we compared the growth rates of HFL-1, MRC-5, LL97A, HLF-a, A549 and H1703 for 96 h to serve as a reference for the following experiments, firstly. As shown in Figure 3a and Table 1, the growth rates of NSCLC cells (A549 and H1703) and human embryonic lung fibroblasts (HFL-1 and MRC-5) were significantly higher than LL97A and HLF-a. Therefore, we continued to select MRC-5 and HLF-a as the objects with different growth rates for effects of LPA stimulating fibroblasts proliferation at different concentrations, representatively. And considering the interference of FBS on the LPA interaction effect, we chose serum-free media for these experiments. Interestingly, both MRC-5 and HLF-a proliferated significantly and showed a concentration-dependent increase when stimulated by LPA, except 20 μM (Figure 3b). Furthermore, we silenced the expression of LPAR1 or B7-H3 simultaneously under the stimulation of LPA concentration of 10 μM in the two fibroblasts, and the results showed that

the proliferation effect induced by LPA was significantly Inhibited (Figure 3c). The same results were obtained in our subsequent experiments using Ki16425 (Figure 3d). These findings demonstrated that LPA induced fibroblasts proliferation that effect could be inhibited by blocking LPAR1 signaling pathway or silencing LPAR1 or B7-H3 expression.

Knocking out CD276 (B7-H3) or LPAR1 prevented CAFs from promoting lung cancer cell proliferation in coculture system

To verify the effects of fibroblasts on the proliferation of NSCLC cells in vitro, we initially cultured A549 and H1703 with conditioned media (CM) obtained from MRC-5 and HLF-a, correspondingly. As shown in Figure 4a, both CM derived from fibroblasts have the potential to encourage the proliferation of A549 and H1703, but the CM derived from HLF-a significantly had a stronger promoting effect. Although the underlying molecular mechanism remains ill-

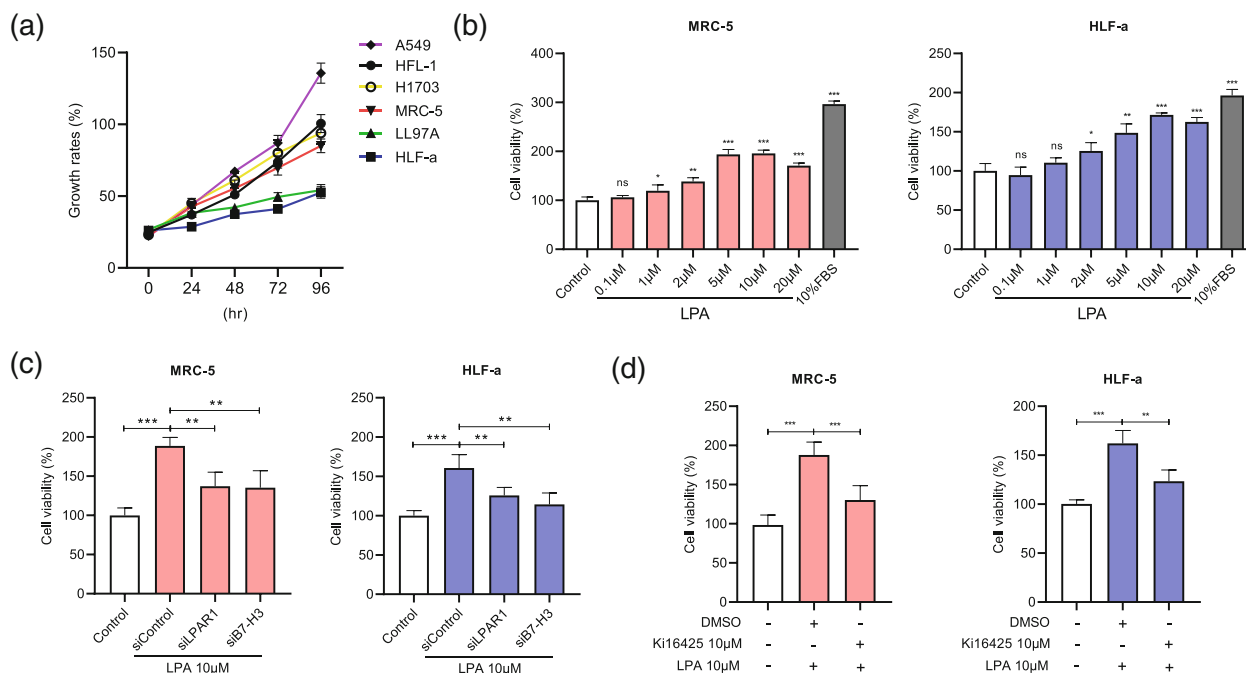


FIGURE 3 Silencing of LPAR1 or CD276 (B7-H3) inhibited lysophosphatidic acid (LPA)-stimulated fibroblast proliferation. (a) Proliferation data showed that the difference of growth rates of HFL-1, MRC-5, LL97A, HLF-a, A549 and H1703 in 10% fetal bovine serum (FBS) media. (b) Proliferation data showed that after 72 h of MRC-5 and HLF-a cells in the presence of LPA 18:1 concentration gradient; MEM media with 10% FBS was a positive control. (c) Proliferation data showed that after 72 h of MRC-5 and HLF-a cells treated with LPA 18:1 (10 μM) with or without transfected with 50 nM siRNAs of LPAR1 or B7-H3. (d) Proliferation data showed that after 72 h of MRC-5 and HLF-a cells treated with or without LPA 18:1 (10 μM) and Ki16425 (10 μM). Data represent mean ± SD. Significance compared to negative control was assessed by two-sided *t*-test. ****p* < 0.001; ***p* < 0.01; **p* < 0.05; ns, no significance.

TABLE 1 The growth rates of HFL-1, MRC-5, LL97A, HLF-a, A549 and H1703 in 10% fetal bovine serum media.

	Cell viability (%) a		
	48 h	72 h	96 h
HFL-1	51.04 ± 1.75	73.78 ± 3.48	100.00 ± 5.12
HLF-a	37.41 ± 2.39**	41.02 ± 2.37***	52.51 ± 3.31***
LL97A	42.19 ± 2.04**	49.45 ± 2.04**	54.25 ± 3.19***
MRC-5	55.43 ± 4.68 ^{ns}	69.71 ± 4.13 ^{ns}	85.01 ± 3.97*
A549	67.14 ± 1.52***	87.02 ± 4.35*	135.65 ± 5.75**
H1703	61.12 ± 4.33*	80.07 ± 7.32 ^{ns}	93.88 ± 6.52 ^{ns}

Abbreviation: ns, no significance.

^aData represent mean ± SD. Significance compared to HFL-1 was assessed by two-sided *t*-test.

****p* < 0.001.

***p* < 0.01.

**p* < 0.05.

defined, A549 was more sensitive to CM derived from HLF-a and the CM derived from tumor cells failed to induce fibroblasts proliferation (Figure S2). These findings are consistent with other tumors model that have been reported.²¹ To further explore the roles of LPAR1 and B7-H3 in promoting lung tumor cell proliferation in CAFs. We then used CRISPR-Cas9 gene editing system to knock out LPAR1 or CD276 in HLF-a and then obtained two engineered fibroblasts (HLF-a^{CD276-/-} and HLF-a^{LPAR1-/-}). We also

cocultured A549-eGFP-Puro with engineered HLF-a at a ratio of 1:5 (Figure 4b).²² As shown in Figure 4c,d, coculture of HLF-a^{wt} significantly promoted the proliferation of A549-eGFP-Puro compared with monoculture. Meanwhile, HLF-a^{CD276-/-} or HLF-a^{LPAR1-/-} coculture showed significant proliferation inhibition on A549-eGFP-Puro.

Knocking out CD276 (B7-H3) or LPAR1 inhibited CAFs promotion of lung tumor growth in xenograft models

To further clarify the importance of B7-H3 and LPAR1 in promoting tumor growth of CAFs in vivo, A549 and H1703 were injected alone or coinjected with HLF-a^{wt}, HLF-a^{CD276-/-} or HLF-a^{LPAR1-/-} by 1:5 ratio into the lower back subcutaneous skin of immunodeficient mice, respectively. As shown in Figure 5a-c, wild-type HLF-a significantly promoted the tumor growth of NSCLC. In contrast, HLF-a^{CD276-/-} or HLF-a^{LPAR1-/-} coinjected significantly inhibited tumor proliferation. In addition, wild-type HLF-a promoted H1703 tumor proliferation and was associated with a worse survival rate in mice (Figure 5d). Moreover, immunohistochemical results of tumors also showed that the mixed inoculation of wild-type rather than knockout LPAR1 or B7-H3 fibroblasts also increased the degree of A549 tumor fibrosis, which was also supported by a significant increase

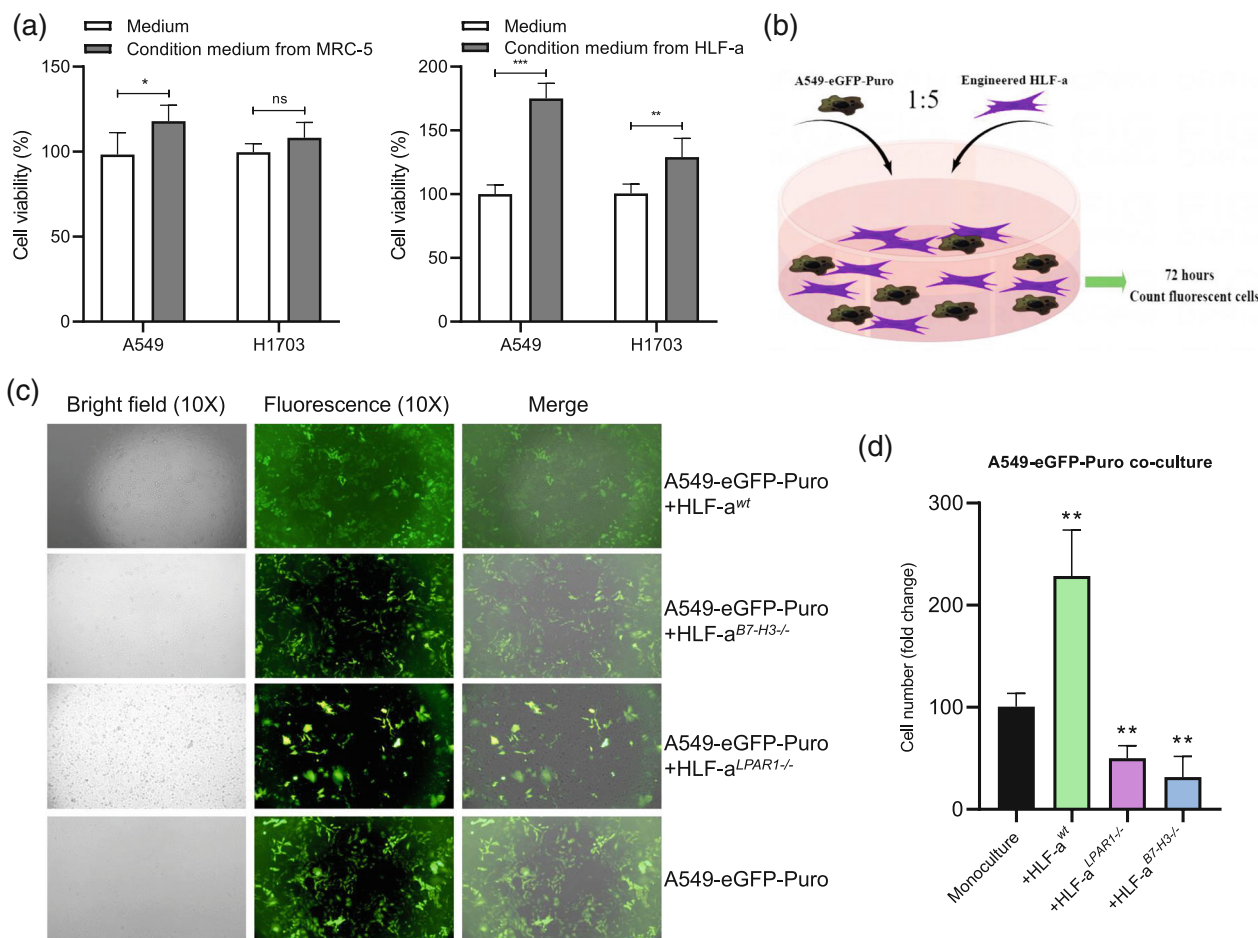


FIGURE 4 Knocking out CD276 (B7-H3) or LPAR1 prevented cancer-associated fibroblasts (CAFs) from promoting lung cancer cell proliferation in coculture system. (a) Proliferation data showed that after 72 h of A549 and H1703 incubated in conditioned media (CM). The CM was Dulbecco's modified Eagle medium (DMEM) with 10% fetal bovine serum (FBS) after incubation of MRC-5 or HLF-a for 48 h. (b) Schematic diagram of coculture model. (c) Fluorescence images of coculture and monoculture after 72 h. (d) Relative quantitative analysis of fluorescent cells in four random fields of view described in (c). Data represent mean \pm SD. Significance compared to negative control was assessed by two-sided *t*-test. ****p* < 0.001; ***p* < 0.01; **p* < 0.05; ns, no significance.

in Sirian red staining of total collagen and CAFs labeled by fibroblast activation protein (FAP) and α -smooth muscle actin (α -SMA) (Figure 5e). Collectively, these data demonstrated that B7-H3 and LPAR1 are essential molecules for CAFs to promote lung tumor growth, and the absence of B7-H3 or LPAR1 could lead to CAFs inhibiting tumor proliferation.

DISCUSSION

The TME consists of ECM components and a variety of cell types, such as tumor cells, immune cells, fibroblasts, among others.¹ As a critical building component of TME, CAFs have previously been found to deposit ECM, modulate metabolism, construct an immunosuppressive environment, and promote tumor growth and invasion.^{2,23} Several studies have linked increased LPA signaling with the biological events related to carcinogenesis and tumor progression, such

as malignant transformation, increased cancer stem cell proliferation, enhanced invasion and metastasis, reprogramming of tumor and metastatic microenvironments, and development of therapy resistance.^{24–26} However, there are few studies on whether and how LPA regulates fibroblasts in the TME. In particular, it is unclear how CAFs interact with tumor cells and by what mechanism(s) LPA regulate checkpoint signaling of CAFs. In this study, we found and confirmed that LPAR1 and CD276 (B7-H3) are generally highly expressed in fibroblasts with strong correlation for the first time. Meanwhile, LPA, as a bioactive phospholipid abnormally secreted under pathological conditions, promoted the expression of B7-H3 through its receptor LPAR1 and stimulated fibroblasts proliferation. Blocking LPAR1 signaling pathway or silencing LPAR1 or B7-H3 expression could also inhibit the proliferation effect by LPA stimulation. Moreover, subsequent in vitro and in vivo investigations demonstrated that LPAR1 and B7-H3 were indispensable for CAFs to promote NSCLC proliferation.

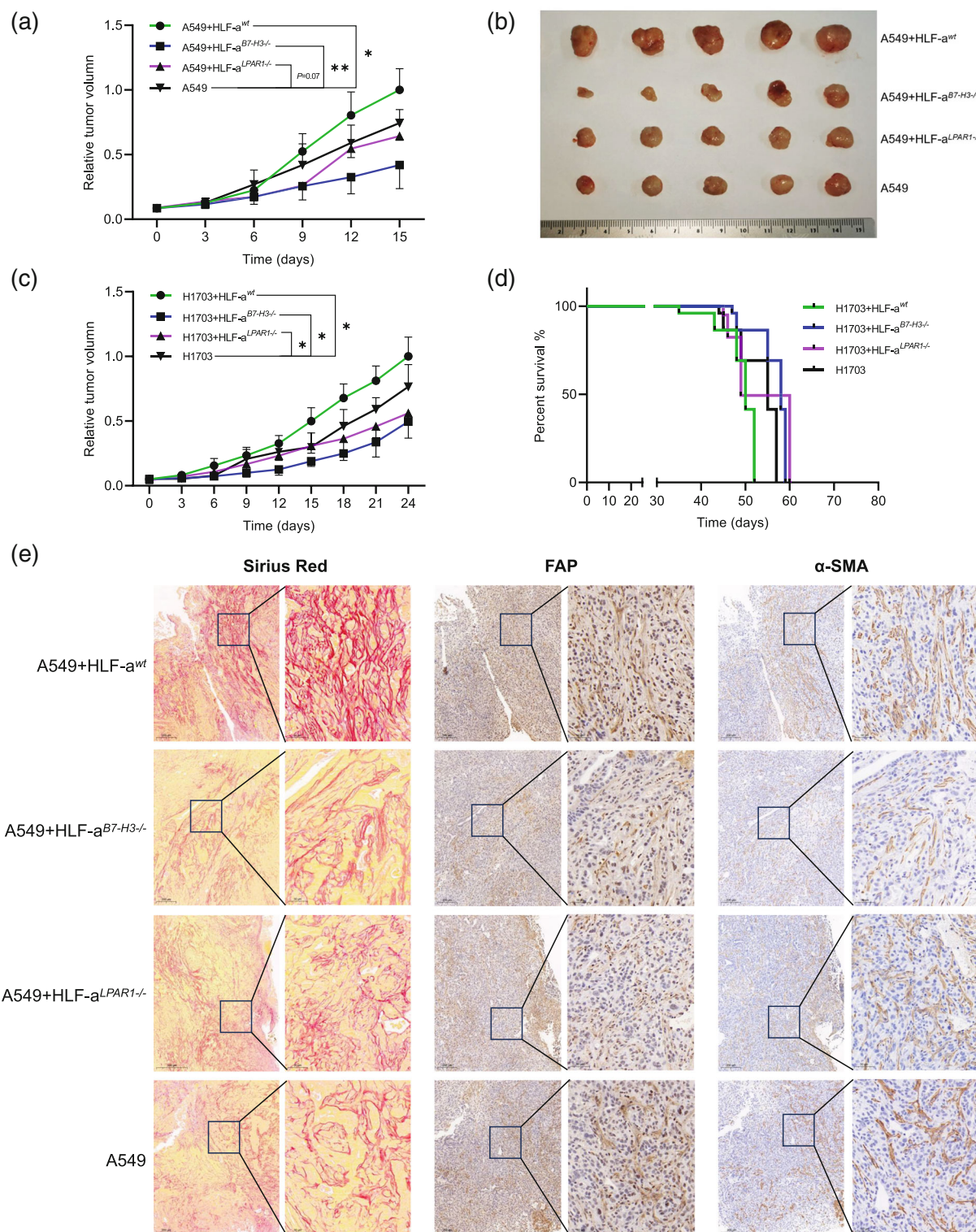


FIGURE 5 Knocking out CD276 (B7-H3) or LPAR1 inhibited cancer-associated fibroblasts (CAFs) promotion of lung tumor growth in xenograft models. (a) Tumor volumes from A549 cells upon subcutaneous transplantation into NOD-SCID hosts, with or without fibroblasts in a 1:5 ratio ($n = 5$). (b) Mice tumor photograph of (a). (c) Tumor volumes from H1703 cells upon subcutaneous transplantation into NOD-SCID hosts, with or without fibroblasts in a 1:5 ratio ($n = 5$). (d) Overall survival curves of the same mice described in (c). (e) Representative immunohistochemical sections image from the same mice described in (a), left panel for Sirian red staining, middle and right panels stained for FAP and α -SMA, respectively. Data represent mean \pm SD. Stastical significance was assessed by two-sided t -test. *** $p < 0.001$; ** $p < 0.01$; * $p < 0.05$; ns, no significance.

B7-H3 is an important member of the B7 family of check point molecules.²⁷ Many studies have confirmed that B7-H3 plays a crucial role in adaptive immunity by regulating T cell function.²⁸ B7-H3 is widely expressed in primary malignant tumors, and studies have also shown that B7-H3 plays an important role in tumor progression in addition to immune escape, including proliferation and migration, angiogenesis, and gene regulation through epigenetic modifications.²⁹ The above findings make B7-H3 a promising new target for immunotherapy after PD-L1 and CTLA-4. To date, more than a dozen clinical trials targeting B7-H3 have been initiated. Examples include enoblituzumab (MGA271), a humanized and Fc-engineered antibody for prostate cancer and NSCLC, ifinatamab (DS-7300), which is in phase II clinical trials for previously treated patients with extensive-stage small cell lung cancer (SCLC), and several ongoing CAR-T clinical trials targeting B7-H3 (NCT05341492; NCT03198052 etc.).^{30,31} Interestingly, B7-H3 has been shown to have a dual function of costimulation and coinhibition.²⁷ This is very similar to the current functional certification for CAFs. However, the link between LPA and B7-H3 is not clear in CAFs. Functionally, it has been reported that LPA induces the glycolysis transition of normal fibroblasts to CAFs by upregulating HIF1 α levels.¹⁸ Moreover, B7-H3 promotes aerobic glycolysis in oral squamous carcinoma via PI3K/Akt/mTOR pathway and promotes tumor growth.³² Our study further confirmed and supplemented that LPA upregulates the expression of B7-H3 in CAFs through its receptor LPAR1, and the metabolic reprogramming of CAFs caused by B7-H3 overexpression is a key factor in promoting tumor progression.³³

While CAFs reside in almost all solid tumors, their contribution to stromal populations varies by types of cancer. For example, breast, pancreatic and lung cancers display high CAFs density, whereas brain, kidney and ovarian cancers display a relatively lower CAFs density.³⁴ NSCLC with high CAFs density and high incidence was finally selected as the research object in this study. Moreover, for the two most important tissue subtypes of NSCLC, lung adenocarcinoma and lung squamous cell carcinoma, we also selected A549 and H1703 as representatives in the study, despite the lack of certain scientific rigor. Our *in vivo* results are consistent with a previously reported study for intrahepatic cholangiocarcinoma,³⁵ although the ratio of cancer cells to fibroblasts used different. Despite disparities in experimental conditions, the present study observed significant differences between MRC-5 and HLF-a in growth rates, expression of B7-H3, and sensitivity to LPA stimulation. Unfortunately, we were unable to verify these findings using patient-isolated fibroblasts due to ethical and technical issues. The fibroblast cell lines used in our study have been validated in the literature and are extensively employed in various cancer and fibrosis models.^{36–39}

There were certain limitations to our study. The unavailability of sufficient Ki16425 prevented us from examining the effect of blocking the LPAR1 signaling pathway on tumor growth *in vivo*. Furthermore, the lack of uniformed

and precise markers defining CAFs remained a technical challenge.³ Therefore, the isolated and cultured fibroblasts in this study might not be able to capture the full spectrum of CAFs *in vivo* in patient tumors. In addition, due to the lack of cancer gene information databases such as TCGA, it is more difficult to investigate fibroblasts than tumors. Nonetheless, the present findings provide valuable and needed knowledge between LPA and its receptors in regulating check point molecules in fibroblasts, as well as a new insight for the role of CAFs in tumor proliferation.

In conclusion, the current findings in our study fill a knowledge gap between LPA and its receptors in the regulation of checkpoint protein B7-H3 in fibroblasts. For tumors with high CAF density such as NSCLC, it is hoped that the present study will provide new insights into the role of CAFs in tumor proliferation and lead to enhanced treatment outcomes for patients via combination of LPAR1 antagonists and B7-H3 targeting therapies.

AUTHOR CONTRIBUTIONS

Conceptualization: Meng and Wang; Study design and execution: Meng, Yin and Lu; Data analysis and summary: Meng and Wang; Writing – original draft: Meng and Zhang; Writing – review and editing: Meng, Zhang and Wang. All authors have read and agreed to the published version of the manuscript.

FUNDING INFORMATION

This research was supported by the National Natural Science Foundation of China (no. 81773044) and (no. 82273193); Social Development Project of Jiangsu Province (BE2019657).

CONFLICT OF INTEREST STATEMENT

All authors declare no conflict of interest.

DATA AVAILABILITY STATEMENT

Sets of data or summaries generated during the present study are available from the corresponding author upon reasonable request.

ORCID

Fanyi Meng  <https://orcid.org/0009-0009-5792-4531>

REFERENCES

1. Bejarano L, Jordao MJC, Joyce JA. Therapeutic targeting of the tumor microenvironment. *Cancer Discov.* 2021;11:933–59. <https://doi.org/10.1158/2159-8290.CD-20-1808>
2. Sahai E, Astsaturov I, Cukierman E, DeNardo DG, Egeblad M, Evans RM, et al. A framework for advancing our understanding of cancer-associated fibroblasts. *Nat Rev Cancer.* 2020;20:174–86. <https://doi.org/10.1038/s41568-019-0238-1>
3. Piersma B, Hayward MK, Weaver VM. Fibrosis and cancer: a strained relationship. *Biochim Biophys Acta Rev Cancer.* 2020;1873:188356. <https://doi.org/10.1016/j.bbcan.2020.188356>
4. Attieh Y, Clark AG, Grass C, Richon S, Pocard M, Mariani P, et al. Cancer-associated fibroblasts lead tumor invasion through integrin-beta3-dependent fibronectin assembly. *J Cell Biol.* 2017;216:3509–20. <https://doi.org/10.1083/jcb.201702033>

5. Yoon H, Tang CM, Banerjee S, Delgado AL, Yebra M, Davis J, et al. TGF- β -mediated transition of resident fibroblasts to cancer-associated fibroblasts promotes cancer metastasis in gastrointestinal stromal tumor. *Oncogenesis*. 2021;10:13. <https://doi.org/10.1038/s41389-021-00302-5>
6. Yoshida GJ. Regulation of heterogeneous cancer-associated fibroblasts: the molecular pathology of activated signaling pathways. *J Exp Clin Cancer Res*. 2020;39:112. <https://doi.org/10.1186/s13046-020-01611-0>
7. Kalluri R. The biology and function of fibroblasts in cancer. *Nat Rev Cancer*. 2016;16:582–98. <https://doi.org/10.1038/nrc.2016.73>
8. Hu G, Xu F, Zhong K, Wang S, Huang L, Chen W. Activated tumor-infiltrating fibroblasts predict worse prognosis in breast cancer patients. *J Cancer*. 2018;9:3736–42. <https://doi.org/10.7150/jca.28054>
9. Zhang H, Yue X, Chen Z, Liu C, Wu W, Zhang N, et al. Define cancer-associated fibroblasts (CAFs) in the tumor microenvironment: new opportunities in cancer immunotherapy and advances in clinical trials. *Mol Cancer*. 2023;22:159. <https://doi.org/10.1186/s12943-023-01860-5>
10. Loeffler M. Targeting tumor-associated fibroblasts improves cancer chemotherapy by increasing intratumoral drug uptake. *J Clin Investig*. 2006;116:1955–62. <https://doi.org/10.1172/jci26532>
11. Lo A, Wang L-CS, Scholler J, Monslow J, Avery D, Newick K, et al. Tumor-promoting Desmoplasia is disrupted by depleting FAP-expressing stromal cells. *Cancer Res*. 2015;75:2800–10. <https://doi.org/10.1158/0008-5472.Can-14-3041>
12. Geraldo LHM, Spohr T, Amaral RFD, Fonseca A, Garcia C, Mendes FA, et al. Role of lysophosphatidic acid and its receptors in health and disease: novel therapeutic strategies. *Signal Transduct Target Ther*. 2021;6:45. <https://doi.org/10.1038/s41392-020-00367-5>
13. Yung YC, Stoddard NC, Chun J. LPA receptor signaling: pharmacology, physiology, and pathophysiology. *J Lipid Res*. 2014;55:1192–214. <https://doi.org/10.1194/jlr.R046458>
14. Tager AM, LaCamera P, Shea BS, Campanella GS, Selman M, Zhao Z, et al. The lysophosphatidic acid receptor LPA1 links pulmonary fibrosis to lung injury by mediating fibroblast recruitment and vascular leak. *Nat Med*. 2008;14:45–54. <https://doi.org/10.1038/nm1685>
15. Mathew D, Torres RM. Lysophosphatidic acid is an inflammatory lipid exploited by cancers for immune evasion via mechanisms similar and distinct from CTLA-4 and PD-1. *Front Immunol*. 2020;11:531910. <https://doi.org/10.3389/fimmu.2020.531910>
16. Turner JA, Fredrickson MA, D'Antonio M, Katsnelson E, MacBeth M, Van Gulick R, et al. Lysophosphatidic acid modulates CD8 T cell immunosurveillance and metabolism to impair anti-tumor immunity. *Nat Commun*. 2023;14:3214. <https://doi.org/10.1038/s41467-023-38933-4>
17. Mazzocca A, Dituri F, Lupo L, Quaranta M, Antonaci S, Giannelli G. Tumor-secreted lysophosphatidic acid accelerates hepatocellular carcinoma progression by promoting differentiation of peritumoral fibroblasts in myofibroblasts. *Hepatology*. 2011;54:920–30. <https://doi.org/10.1002/hep.24485>
18. Radhakrishnan R, Ha JH, Jayaraman M, Liu J, Moxley KM, Isidoro C, et al. Ovarian cancer cell-derived lysophosphatidic acid induces glycolytic shift and cancer-associated fibroblast-phenotype in normal and peritumoral fibroblasts. *Cancer Lett*. 2019;442:464–74. <https://doi.org/10.1016/j.canlet.2018.11.023>
19. Shi J, Jiang D, Yang S, Zhang X, Wang J, Liu Y, et al. LPAR1, correlated with immune infiltrates, is a potential prognostic biomarker in prostate cancer. *Front Oncol*. 2020;10:846. <https://doi.org/10.3389/fonc.2020.00846>
20. Mills GB, Moolenaar WH. The emerging role of lysophosphatidic acid in cancer. *Nat Rev Cancer*. 2003;3:582–91. <https://doi.org/10.1038/nrc1143>
21. Yang X, Lin Y, Shi Y, Li B, Liu W, Yin W, et al. FAP promotes immunosuppression by cancer-associated fibroblasts in the tumor microenvironment via STAT3-CCL2 signaling. *Cancer Res*. 2016;76:4124–35. <https://doi.org/10.1158/0008-5472.CAN-15-2973>
22. Auciello FR, Bulusu V, Oon C, Tait-Mulder J, Berry M, Bhattacharyya S, et al. A stromal Lysolipid-Autotaxin signaling Axis promotes pancreatic tumor progression. *Cancer Discov*. 2019;9:617–27. <https://doi.org/10.1158/2159-8290.CD-18-1212>
23. Feng B, Wu J, Shen B, Jiang F, Feng J. Cancer-associated fibroblasts and resistance to anticancer therapies: status, mechanisms, and countermeasures. *Cancer Cell Int*. 2022;22:166. <https://doi.org/10.1186/s12935-022-02599-7>
24. Tigyi GJ, Yue J, Norman DD, Szabo E, Balogh A, Balazs L, et al. Regulation of tumor cell – microenvironment interaction by the autotaxin-lysophosphatidic acid receptor axis. *Adv Biol Regul*. 2019;71:183–93. <https://doi.org/10.1016/j.jbior.2018.09.008>
25. Benesch MGK, Yang Z, Tang X, Meng G, Brindley DN. Lysophosphatidate signaling: the tumor Microenvironment's new nemesis. *Trends Cancer*. 2017;3:748–52. <https://doi.org/10.1016/j.trecan.2017.09.004>
26. Leblanc R, Peyruchaud O. New insights into the autotaxin/LPA axis in cancer development and metastasis. *Exp Cell Res*. 2015;333:183–9. <https://doi.org/10.1016/j.yexcr.2014.11.010>
27. Ni L, Dong C. New B7 family checkpoints in human cancers. *Mol Cancer Ther*. 2017;16:1203–11. <https://doi.org/10.1158/1535-7163.MCT-16-0761>
28. Picarda E, Ohaegbulam KC, Zang X. Molecular pathways: targeting B7-H3 (CD276) for human cancer immunotherapy. *Clin Cancer Res*. 2016;22:3425–31. <https://doi.org/10.1158/1078-0432.CCR-15-2428>
29. Li P, Yang Y, Jin Y, Zhao R, Dong C, Zheng W, et al. B7-H3 participates in human salivary gland epithelial cells apoptosis through NF- κ B pathway in primary Sjogren's syndrome. *J Transl Med*. 2019;17:268. <https://doi.org/10.1186/s12967-019-2017-x>
30. Liu C, Zhang G, Xiang K, Kim Y, Lavoie RR, Lucien F, et al. Targeting the immune checkpoint B7-H3 for next-generation cancer immunotherapy. *Cancer Immunol Immunother*. 2022;71:1549–67. <https://doi.org/10.1007/s00262-021-03097-x>
31. Shenderov E, De Marzo AM, Lotan TL, Wang H, Chan S, Lim SJ, et al. Neoadjuvant enoblituzumab in localized prostate cancer: a single-arm, phase 2 trial. *Nat Med*. 2023;29:888–97. <https://doi.org/10.1038/s41591-023-02284-w>
32. Li Z, Liu J, Que L, Tang X. The immunoregulatory protein B7-H3 promotes aerobic glycolysis in oral squamous carcinoma via PI3K/Akt/mTOR pathway. *J Cancer*. 2019;10:5770–84. <https://doi.org/10.7150/jca.29838>
33. Eisenberg L, Eisenberg-Bord M, Eisenberg-Lerner A, Sagi-Eisenberg R. Metabolic alterations in the tumor microenvironment and their role in oncogenesis. *Cancer Lett*. 2020;484:65–71. <https://doi.org/10.1016/j.canlet.2020.04.016>
34. Smith NR, Baker D, Farren M, Pommier A, Swann R, Wang X, et al. Tumor stromal architecture can define the intrinsic tumor response to VEGF-targeted therapy. *Clin Cancer Res*. 2013;19:6943–56. <https://doi.org/10.1158/1078-0432.CCR-13-1637>
35. Lin Y, Li B, Yang X, Cai Q, Liu W, Tian M, et al. Fibroblastic FAP promotes intrahepatic cholangiocarcinoma growth via MDSCs recruitment. *Neoplasia*. 2019;21:1133–42. <https://doi.org/10.1016/j.neo.2019.10.005>
36. Wang Y, Sima X, Ying Y, Huang Y. Exogenous BMP9 promotes lung fibroblast HFL-1 cell activation via ALK1/Smad1/5 signaling in vitro. *Exp Ther Med*. 2021;22:728. <https://doi.org/10.3892/etm.2021.10160>
37. Peng J, Li S, Li B, Hu W, Ding C. Exosomes derived from M1 macrophages inhibit the proliferation of the A549 and H1299 lung cancer cell lines via the miRNA-let-7b-5p-GNG5 axis. *PeerJ*. 2023;11:e14608. <https://doi.org/10.7717/peerj.14608>
38. Velazquez-Enriquez JM, Ramirez-Hernandez AA, Navarro LMS, Reyes-Avendano I, Gonzalez-Garcia K, Jimenez-Martinez C, et al. Proteomic analysis reveals differential expression profiles in idiopathic pulmonary fibrosis cell lines. *Int J Mol Sci*. 2022;23:5032. <https://doi.org/10.3390/ijms23095032>

39. He J, Peng H, Wang M, Liu Y, Guo X, Wang B, et al. Isoliquiritigenin inhibits TGF-beta1-induced fibrogenesis through activating autophagy via PI3K/AKT/mTOR pathway in MRC-5 cells. *Acta Biochim Biophys Sin* (Shanghai). 2020;52:810–20. <https://doi.org/10.1093/abbs/gmaa067>

SUPPORTING INFORMATION

Additional supporting information can be found online in the Supporting Information section at the end of this article.

How to cite this article: Meng F, Yin Z, Lu F, Wang W, Zhang H. Disruption of LPA-LPAR1 pathway results in lung tumor growth inhibition by downregulating B7-H3 expression in fibroblasts. *Thorac Cancer*. 2024;15(4):316–26. <https://doi.org/10.1111/1759-7714.15193>